Local Monomer Activation Model for Phase Behavior and Calorimetric Properties of LCST Gel-Forming Polymers

Francisco J. Solis,*,† Rachael Weiss-Malik,‡ and Brent Vernon‡

Integrated Natural Sciences, Arizona State University West, Phoenix, Arizona 85069, and The Harrington Department of Bioengineering, Arizona State University, Tempe, Arizona 85287

Received October 11, 2004; Revised Manuscript Received January 31, 2005

ABSTRACT: We investigate the phase diagrams and calorimetric signatures of gel-forming polymers with a lower critical solution temperature (LCST). We construct a model that captures many of the observed properties of this type of polymer. The model assumes the existence of a sharp internal conversion, at a characteristic temperature T^*, in which monomers are activated from effectively hydrophilic to associative-hydrophobic states. The location of the gel transition is determined by Flory's model of gelation, while phase separation of polymer and solvent is determined by assuming that the effective immiscibility χ parameter is generated solely from gel-forming contacts. The resulting phase diagrams exhibit an immiscibility loop and a gel−sol boundary. At low temperatures both the phase and the sol−gel boundaries are almost independent of concentration. The gel transition does not produce a signature in the calorimetric properties (heat capacities at constant concentration), but the internal transition produces a clear signal near the gel transition point. The phase separation produces a finite positive jump in the excess heat capacity but is immediately followed by an exothermal feature. We discuss examples of experimentally studied polymeric systems with properties consistent with those of the model.

I. Introduction

Several polymers possess a lower critical solution temperature (LCST) in aqueous solution.[1,2] These polymers in general, and in particular those that form physical thermoreversible gels, have important in vivo medical applications. Because of their phase transition driven by increased temperature, they are often investigated as injectable,[3,4] in vivo-forming,[5,6] biomaterials. In particular, polymers based on *N*-isopropylacrylamide and block copolymers of ethylene glycol[6] have been investigated for injectable, controlled-drug delivery systems for insulin,[7,8] other proteins and peptides,[9] and cancer drugs.[10] These polymers have also been investigated for delivery of living cells[11−14] and for other tissue engineering applications.[3,15−17] The location of the transition temperature as well as the thermodynamic and kinetic properties of these polymers at and near the transition points can be modified by copolymerization.[11−13] A better theoretical quantitative understanding of these properties, and their dependence on the base polymer and the type and degree of copolymerization, can improve the behavior of these systems in currently investigated applications or be used to rationally modify the systems for new applications.

It has been proposed that many of these systems have a LCST because of a *local* structural transition involving the water molecules surrounding specific segments of the polymers in solution.[18−21] At low temperatures water molecules are frozen in place and provide the polymer with a coating that effectively makes it water-soluble. At higher temperatures these molecules unfreeze, allowing associative contacts between the newly exposed monomers. Associations of these freed monomers lead to the formation of a gel as well as an eventual phase separation (synerisis). Figure 1 shows a schematic representation of the three states considered in this theory: monomers with associated water, monomers that have released the associated water and that we will refer to as *activated*, and associated pairs of activated monomers. The model presented in this paper uses this proposal as its starting point to investigate the phase properties of the LCST gels. We label this theory as one of *local* activation, as it will be assumed that the structural changes in the neighborhood of a monomer or statistic unit (before association) occur independently from those of its neighbors. This assumption allows the use of a two-state description of the activation process.

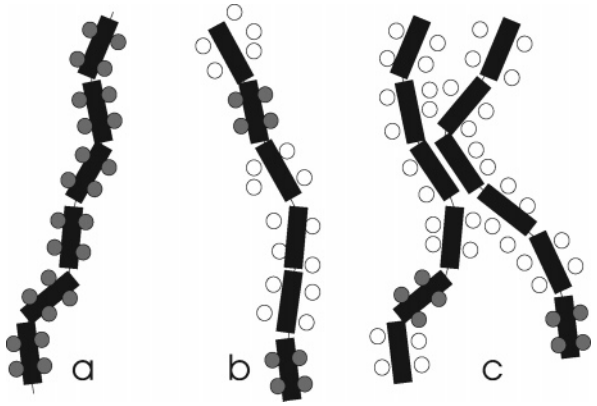

Figure 1. Scheme of the possible states of monomers considered. In (a) a layer of solvent molecules is strongly associated with the monomers (represented by black rectangles). The association is indicated by the shading. The model considers that at higher temperatures each monomer can be found in a state where it is surrounded by either associated or dissociated (in white) solvent molecules. In (b) of the scheme two of the monomers shown still retain strongly associated solvent molecules. Only monomers without associated solvent molecules can participate in the physical bonding with other monomers. In (c) two monomers in different chains form an associative contact.

The change in the state of the monomers from effectively hydrophilic to associative can be modeled and interpreted as arising from different causes, even if end

† Arizona State University West.
‡ Arizona State University.

10.1021/ma047895a CCC: $30.25
Published on Web 04/16/2005

results are similar. The simplest model for this process involves physical association, perhaps by hydrogen bonding, of water molecules and monomers at low temperatures. As the temperature increases, the hydrogen bonds are lost, and the neighboring water molecules become randomly oriented. Models of solutions of hydrogen-bonding substances have been previously discussed,[22,23] although without considerations of gel formation.

A second model, resulting in similar properties of the polymer, suggests that below the LCST point the water that surrounds the polymers is not associated with the monomers but in fact is repelled by them. The repulsion results in very strong hydrogen-bond formation among the water molecules near the monomers. In this model, the activation of associative states of the monomers corresponds to the breakup of the bonds between the surrounding water.[18−21,24−26] A third model has also been proposed in which the changes of the polymers at the transition temperature are related to a coil−globule transition.[27] In this case the model we consider below is not directly applicable, as it assumes only *local* structural changes, but the phase diagram of such substance would share common features with the phase diagram for our model.

The phase diagrams corresponding to both the solute−water and water−water boding models have been explored before, but not in connection with gel formation phenomena. The effective thermodynamic models that can be constructed on the basis of any of these different models of the underlying physics of the phenomena share the common property of a large entropy gain as the either monomer−water, water−water, or monomer−monomer bonds (depending on the model used) are broken.

Recent theoretical studies have focused on the construction of the phase diagrams of gel-forming polymers on the basis of simple theoretical assumptions. The basic theory of gel structure and formation was established long ago by Flory and Stockmayer.[28] More recent works by Rubinstein and Semenov's and Tanaka's groups[29−33] have provided a description of the phase properties of thermoreversible gel-forming polymers by combining Flory's results with simple modeling of the solution properties of these polymers. Other recent theoretical investigations have focused on other aspects of gel structure[34,35] and on atomistic simulations of specific gel-forming polymers.[36]

Erukhimovich and collaborators[30,31] obtained phase diagrams of gel-forming polymers with LCST behavior. To obtain this effect, their model assumed that the association constant for gel contacts has a retrograde temperature dependence of the form $\exp(E/T)$, where E is a positive association energy and T is the temperature. Thus, in this model, the strength of the association increases with temperature. We examine a model with a similar scheme to generate the LCST point, but in which there is a well-defined activation temperature, T^*, above which the monomer interactions are attractive. Our proposed model captures many phenomenological features of LCST gel-forming polymers.

One of the central issues discussed in recent theoretical work is the nature of the gel transition and, in particular, whether it is simply structural rather than thermodynamic. Different models produce, of course, different answers. We will not address this debate here but explicitly use a model that exhibits a purely structural transition. In models that show a true gel phase transition, the phase coexistence region is small, and the overall contribution to the specific heat associated with the transition is also small (even if singular). Furthermore, the assumption of an activation of associative behavior at a given temperature entails a strong dominant behavior of the thermal properties of the system by the activation process, effectively reducing the thermodynamic contribution of the gel formation to a secondary effect. Thus, we expect many of the predictions of the model to persist even if modeling details that modify the transition degree are considered.

The qualitative interpretation of calorimetric experiments on polymers is well established,[37] but identification of signatures that arise from specific theoretical models or common features of families of polymers has only recently been addressed.[38,39] We identify several calorimetric features of the model considered below that are both easily identifiable and explicitly connected with the assumptions used to build the model.

While it is necessary to explicitly include several complex terms in our model's free energy, the model basic idea is rather simple. Once the assumption is made that the major determinant of the behavior of the system is this local internal activation, most of the results of the theory are easy to foresee. The temperatures at which the gelation and (lower) phase separation occur are set by the temperature of the internal conversion and are nearly concentration independent. The main specific heat signal is also directly associated with the monomers' activation.

In many of the proposed applications of these systems, it is implicitly assumed or desired that the crucial features of the polymers, such as the onset of gel formation, be effectively concentration independent over a suitable concentration range. This is a very constraining requirement, and the only way to eliminate concentration dependence is to use a sharp thermal "switch". The strong concentration dependence of the gel formation and phase separation in regular systems is then collapsed into a small range of temperatures above the activation point. This reverse argument shows that these features, observed in concrete systems, require the presence of a local activation and thus justify the basic assumption of the model.

II. Model

We describe the properties of the gel-forming and phase separating polymer by means of a free energy functional F written in terms of three main variables: the volume fraction ϕ, the fraction of monomers activated for association f, and the fraction of activated monomers actually associated Γ. The total free energy is written in terms of three different components as

$$F = F_{\mathrm{in}} + F_{\mathrm{sol}} + F_{\mathrm{as}} \tag{1}$$

As described below, F_{in} reflects the changes in the local state of monomers, F_{sol} is a standard regular solution model functional, and F_{as} is the contribution to the free energy due to the association of activated monomers.

The existence of an LCST point for polymer gels can be interpreted as indicating a sudden change on the monomers from hydrophilic to hydrophobic states, induced by temperature increases. We can model this behavior by a simple two-state model in which the water molecules surrounding a monomer are either tightly

bound to it (or with each other) or present in random orientations in its vicinity. The fraction of inactive, water-bound monomers is $1 - f$, while the fraction of activated monomers is f. As outlined in the Introduction, other physical models can also be described in similar ways. We assume that, on average, there is a negative association energy E that arises from the associations between the local components of the polymer core and its water or solvent environment. The water molecules released from this configurations gain a (mostly rotational) entropy s. In the absence of interactions between monomers, a suitable free energy functional is

$$F_{\text{in}} = Tf\varphi \ln f + T(1-f)\varphi \ln(1-f) + f\varphi(E - Ts) \quad (2)$$

The first two terms of this expression reflect the entropy of choosing a fraction f of activated monomers. The last term is the change in free energy associated with the activation of the monomers. This free energy can be derived from a two-state partition function in which each monomer and its surrounding solvent molecules act independently of each other.[20,25,26] The model can be derived, as mentioned in the Introduction, from different physical pictures. When it is assumed that the entropy and enthalpy changes arise, for the most part, from the rupture of hydrogen bonds between water molecules surrounding the polymer, numerical values for the energies and entropies involved (per water molecule) have been approximately determined by different groups.[20,26]

Minimization of the internal conversion contribution to the free energy F_{in} with respect to the activated fraction f leads to an activated fraction f_0 of noninteracting monomers given by

$$f_0 = (1 + \exp(-s - E/T))^{-1} \quad (3)$$

This population function establishes a characteristic temperature scale T^*, at which half of the monomers have been activated; this is

$$T^* = |E|/s \quad (4)$$

We will consider only the case in which both s and E are large compared to the association energy g (discussed below), so that interactions between polymers affect this population minimally. The sharpness of the transition can be described by the width of the range of temperatures ΔT over which most of the activation takes place. This width is of order

$$\Delta T \sim T^*/s \quad (5)$$

To describe the phase properties of gels, it is useful to model the concentration-dependent properties of the polymers with a regular solution model free energy functional.[29−33,40,41] The contribution of noninteracting chains to the free energy can be taken as

$$F_{\text{sol}} = T\frac{\varphi}{N}\ln\frac{\varphi}{N} + T(1-\varphi)\ln(1-\varphi) \quad (6)$$

In this expression, N is the monomer number, and it is assumed that monomers occupy a single effective statistical site, with volume similar to that of solvent molecules. When there are other interactions involving nonassociating sections of the polymer chain, other terms can be added; for example, a χ parameter term proportional to the square of the concentration and a virial term proportional to the cube of the concentration can be added to the equation.

A fraction f of the monomers is in an associative state, that is, susceptible to form a physical bond with other monomers. Association of a pair of monomers involves a mostly enthalpic change in the free energy by an amount $g < 0$ and a concentration-dependent entropy decrease. These associations produce structures that in Flory's model are all treelike. We define the variable Γ as the fraction of activated monomers that are actually found in associated states. The following free energy density[29−31] F_{as} approximately captures the total change in the free energy due to the formation of the treelike structures:

$$F_{\text{as}} = -T\varphi f\frac{\Gamma}{2}\ln\frac{\varphi}{e} + T\varphi f\left[\frac{\Gamma}{2}\ln\Gamma + (1-\Gamma)\ln(1-\Gamma)\right] + g\varphi f\Gamma \quad (7)$$

This expression estimates the change in free energy for all levels of association Γ in both pre- and postgel regimes. This functional can be written in many equivalent ways. In this form, its terms can be roughly identified with the average change in translational entropy of active monomers arising from associations, with the entropy change due to the actual realization of the associated structure among the many possibilities available, and with the enthalpic changes due to associations, per monomer.

For homogeneous states the total free energy is evaluated by minimizing of the total free energy functional with respect to the fraction of activated monomers f and the fraction of activated monomers that are in effect associated, Γ. Minimization with respect to the associated fraction Γ leads to the mass action law:

$$\frac{\Gamma}{(1-\Gamma)^2} = f\varphi \exp(-2g/T) \quad (8)$$

This expression highlights the fact that Flory's model assumes that the Nf activated monomers per chain effectively act as independent entities.

Minimizing the total free energy with respect to the activated fraction f leads to a simple, and in most cases, small modification of the associated fraction as a function of the temperature. We obtain

$$f = \frac{1}{1 + (1-\Gamma)\exp(-s - E/T)} \quad (9)$$

Evaluation of the total free energy requires the simultaneous solution of eqs 8 and 9 for the associated fraction Γ and activated fraction f. Note that for small concentrations, where there is a small number of associations, we recover the noninteracting activation fraction f_0.

Gelation occurs when the structure formed by the associated polymers percolate throughout the bulk of the system. This condition is satisfied when the associated fraction of monomers is larger than a critical value, $\Gamma > \Gamma_{\text{cr}}$. In the mean-field theory approximation,[28] the critical value is given by

$$\Gamma_{\text{cr}} = \frac{1}{fN - 1} \quad (10)$$

The phase coexistence conditions are determined by the condition that both the chemical potential and the partial pressures of two homogeneous phases acquire equal values at the same temperature. The chemical potential is

$$\mu = \frac{\partial F}{\partial \varphi} \tag{11}$$

while the partial pressure of the monomers is

$$p = -F + \mu\varphi \tag{12}$$

Equilibrium between phases is achieved when for two different concentrations φ_1 and φ_2 we have

$$\mu(T,\varphi_1) = \mu(T,\varphi_2) \tag{13}$$

and

$$p(T,\varphi_1) = p(T,\varphi_2) \tag{14}$$

The phase diagrams exhibited below are obtained by application of this procedure to the free energy F_{tot}.

III. General Properties Predicted by the Model

We consider now the basic properties of the model and how they correspond to the basic phenomenological features of the systems under consideration. We consider the neighborhood of the critical points to identify the limits of insolubility of the polymers and the location of the gel transitions for large polymers.

When the fraction of activated associated monomers is small, $\Gamma \ll 1$, the mass action law equation has the approximate solution

$$\Gamma = f\varphi \exp(-2g/T) \tag{15}$$

Evaluation of the total free energy using this value for the associated fraction leads to the approximate expression for the structural part of the energy as a power series in the volume fraction:

$$F_{as} = T\varphi - \frac{\exp(-2g/T)}{2} Tf^2\varphi^2 + \frac{\exp(-4g/T)}{2} Tf^3\varphi^3 \tag{16}$$

The physical association of monomers can then be understood, at the thermodynamic level, as equivalent to a negative (attractive) contribution to the effective χ parameter and a positive contribution to the third-order virial coefficient w, namely

$$\chi_{as} = -\frac{\exp(-2g/T)}{2} f^2 \tag{17}$$

and

$$w_{as} = 3 \exp(-4g/T) Tf^3 \tag{18}$$

Using the previous expressions, the presence of a critical point in the phase diagram can be determined by simultaneously setting the first and second partial derivatives of the chemical potential to zero. The condition on the first derivative of the chemical potential is

$$\frac{1}{N\varphi} + \frac{1}{1-\varphi} - \exp\left(-\frac{2g}{T}\right) f^2 = 0 \tag{19}$$

while the condition on the second derivative is

$$-\frac{1}{N\varphi^2} + \frac{1}{(1-\varphi)^2} + 3 \exp\left(-\frac{4g}{T}\right) f^3 = 0 \tag{20}$$

It can be shown that solutions to these equations, for the critical temperature T_c and concentration φ_c, satisfy the relations

$$\varphi_c = 2N^{-1/2} \tag{21}$$

and

$$f^2 \exp(-2g/T_c) = 1 + (5/2)N^{-1/2} \tag{22}$$

The general behavior we have imposed on the fraction of activated monomers is such that it is approximately zero for temperatures below T^* and approximately 1 for temperatures above T^* with a sharp increase in the neighborhood of T^*. Therefore, the expression determining the critical temperature has two solutions: an upper T_u and a lower T_l critical temperature.

The upper critical solution temperature is achieved in the regime of highly activated monomers, $f \approx 1$. In this case we have

$$T_u = 4|g|N^{1/2}/5 \tag{23}$$

The lower critical temperature appears when $f < 1$, and $\exp(-g/T_l) = 1/f$. Since the activated monomer fraction changes rapidly in the neighborhood of the activation temperature, a solution for the critical relation always exists near T^* as long as the interaction free energy takes a small value, $|g| < T_l$. Therefore, the simplest approximation is to take the lower critical temperature solution as equal to T^*:

$$T_l = T^* \tag{24}$$

Note that, within the range of parameters considered, the upper critical solution temperature (UCST) occurs at a higher temperature than the lower critical point, and therefore these solutions indicate the presence of an immiscibility loop in the phase diagram. The immiscibility loop disappears when the energy of association is so small that the lack of activation hinders association at low temperatures and entropic effects override the association at higher temperatures. This occurs when the upper and lower critical temperatures are equal, and therefore the loop appears only when the strength of the interaction is larger than the minimum value:

$$|g_{min}| = 5T^*/(4N^{1/2}) \tag{25}$$

Let us now consider the conditions for the formation of a gel. Within the present model, two factors limit this process: the activation of the monomers and the degree of association of the activated monomers. Our previous equations lead then to boundaries of the gel region determined by the condition

$$\frac{1}{fN-1} = f\varphi \exp(-2g/T) \tag{26}$$

with the clear requirement that

$$fN > 1 \tag{27}$$

At temperatures well above the activation temperature T^*, the activated fraction is $f = 1$, and the gel forms for concentrations above a minimum value φ_g given as a function of temperature by

$$\varphi_g = \exp(2g/T)/N \tag{28}$$

At lower temperatures, the obstruction to gel formation is the lack of sufficient activated monomers. Requiring that the activated fraction be $f > 1/N$ and expanding the activated fraction in powers of the exponential $\exp(-T^*)$, we obtain a lower bound for the temperature at which the gel can be found, T_g, as

$$T_g = T^*\left[1 - \frac{T^*}{|E|}\ln(N)\right] \tag{29}$$

This temperature lies below the immiscibility loop, but the boundary set by φ_g will often overlap with the loop and give rise to phase coexistence between sol and gel phases.

It is also of interest to determine the region within the phase where the formation of large but finite aggregates occurs. Experimentally, these states are easily observable as visible light is strongly scattered from them. For characterization purposes, it is useful to identify this condition, the "milky" states, within the phase diagrams. A simple estimate of the location of the phase diagram region in which these states can be found is obtained by considering again the case of incipient association, when the number of active monomers in the system is at least one, or $f = 1/N$. At low temperatures, association of active monomers is almost assured, and therefore we can expect their appearance for all temperatures above T_g, but at concentrations at which a gel is not formed.

Calorimetric experiments measure the specific heat of samples of given concentration. It is straightforward to calculate the (constant volume) heat capacity of the model by the basic definition

$$C_v = -T\left.\frac{\partial^2 F}{\partial T^2}\right|_{\varphi,V} \tag{30}$$

According to our conventions, this is a specific heat per unit volume. The heat capacity due to the solvent properties of the system, as reflected in the functional F_{sol}, is zero outside the immiscibility loop. Experimentally, it is often the case that a nonzero background contribution can be identified and subtracted from the total heat capacity. Near the gel transition, and below the lower critical point, it is easy to see that the contribution to the heat capacity due to the internal conversion from inactive to associative monomers is much larger than the heat capacity contribution from association. The heat capacity from internal conversion is approximately given by

$$\Delta C_v = \varphi f(1-f)\frac{E^2}{T^2} \tag{31}$$

Clearly, the heat capacity is strongly peaked at the mid-conversion point, $f = 1/2$, that occurs near the temperature T^*. Since the activated fraction has only a weak dependence on the concentration, we conclude from this expression that the excess heat capacity per mole of monomer, proportional to $\Delta C_v/\varphi$, is almost concentration independent. This particular form of the specific heat is, of course, typical of two-state systems,[42] and it is one of the main characteristics of systems that exhibit a strong hydrophobic transition.[26]

The contribution to the specific heat arising from association, while much smaller than that of internal conversion, becomes relevant in the temperature range of the immiscibility loop.

In calorimetric probes, forward or backward heating at a fixed concentration may imply passage through the immiscibility region. In such case, the total entropy of a system with concentration ϕ at a temperature T inside the immiscibility region is given by

$$S = xS_1 + (1-x)S_2 \tag{32}$$

where S_1 and S_2 are the entropies at the concentrations φ_1 and φ_2 (with $\varphi_1 < \varphi_2$) that are the limits of the coexistence region. The volume fraction x for the state with concentration φ_1 is

$$x = \frac{\varphi_2 - \varphi}{\varphi_2 - \varphi_1} \tag{33}$$

The heat capacity inside this region can be written as

$$C_v = Tx\left.\frac{dS}{dT}\right|_1 + T(1-x)\left.\frac{dS}{dT}\right|_2 \tag{34}$$

where the total derivatives of the entropy with respect to temperature are evaluated along the trajectories, in state space, of the coexisting states $\varphi_1(T)$ and $\varphi_2(T)$. These can be written explicitly as

$$\left.\frac{dS}{dT}\right|_a = \frac{\partial S}{\partial T} + \left(\frac{\partial S}{\partial \varphi} - \frac{S_2 - S_1}{\varphi_2 - \varphi_1}\right)\frac{\partial \varphi_a}{\partial T} \tag{35}$$

On entrance to the immiscibility region from below, it can be shown that the extra terms in the entropy derivative immediately take a nonzero positive value, so that the total heat capacity is discontinuous with a positive jump. On exit, at higher temperature, from the coexistence region, there is a second discontinuity jump, this time negative. However, as we show below in concrete examples, in between these two temperatures the excess heat capacity associated with the passage through the immiscibility region exhibits a strong exothermic behavior, $\Delta C_v < 0$, near the low-temperature transition. The specific expressions for the entropy shown above allow an easier calculation of the calorimetric properties of the system since they directly identify and determine the value of the discontinuities.

IV. Phase Diagrams

To exhibit the recovery of important phenomenological features of actual geling systems from the model, we present a small sample set of phase diagrams obtained by using different values of parameters in the model. In Figure 2, we show four sample phase diagrams. In these, the immiscibility region is shaded, while the boundary between gel and sol states is marked with a solid line. Homogeneous states inside the coexistence region are unstable, but we nevertheless indicate the putative gel or sol conditions for these unstable states by extending the sol−gel boundary to states inside this region. For all the cases considered in the figure we use a monomer number $N = 1000$, but note that the asymptotic limits noted above for the critical

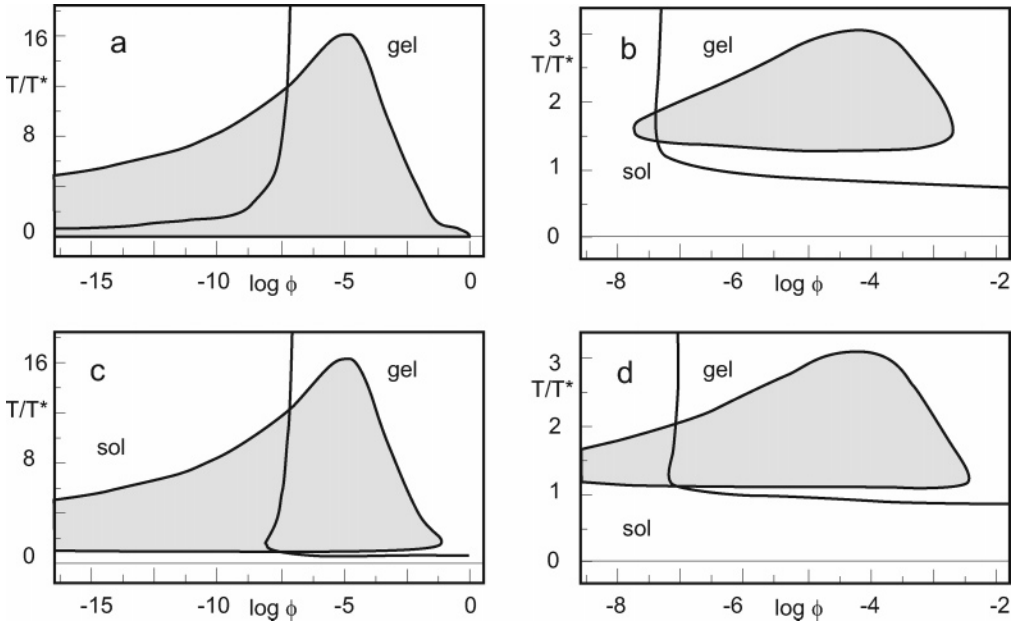

Figure 2. Four examples of phase diagrams for different values of the model parameters. Panel (a) serves as reference, and it is the prediction of a purely associative model with association energy between monomers $g = -1.0$ and no interaction between monomers and solvent. In all diagrams the shaded area is the coexistence region, and the solid line separates sol and gel states. Inside the coexistence region the separation indicates the gel or sol condition of the meta- or unstable states. Panel (b) shows the phase diagram for the case where $s = 10.0$, $E = -10.0T^*$, and $g = -1.0T^*$. The scaling of the temperature coordinate by T^* effectively matches the behavior at high temperature to the case in panel (a). At temperatures below the activation of monomers $T < T^*$ the system is again in a homogeneous state for all concentrations. Panel (c) shows results for $s = 10.0$, $E = -10.0T^*$, and $g = -0.3T^*$. In this case the coexistence region is much reduced. Panel (d) shows results for the case where $s = 20.0$, $E = -20.0T^*$, and $g = -0.3T^*$. The change in parameters from the case (c) produces a much sharper internal transition and the bottom boundary of the coexistence region becomes more closely identified with the internal transition temperature T^*.

points are achieved at even larger values of $N \sim 10\,000$. The vertical axis in the activated cases (b–d) is the scaled temperature T/T^*, and the logarithmic horizontal axis is the concentration φ. Frame a shows the results of the regular Flory's theory when no activation is required and the monomers can associate at all temperatures with an association energy $g = -1.0$ (so as to match the reduced scale in frame b). Frame b uses $g = -1.0T^*$, $s = 10.0$, and $E = -10.0T^*$ and clearly exhibits both a gel and phase transition in the neighborhood of T^*. The scale of the plot was chosen to make comparison with the non-LCST case of part a simpler. Frame c shows the results for $g = -0.2T^*$, $s = 10.0$, and $E = -10.0T^*$, and frame d presents a similar case, but with a sharper transition obtained from $g = -0.2T^*$, $s = 20.0$, and $E = -20.0T^*$. At low concentrations, the fraction of activated monomers has the noninteracting value f_0 and is independent of concentration. These activated fractions are shown in Figure 3 for the pairs of values of $s = 10$, $E = -10T^*$ and $s = 20$, $E = -20T^*$. The first pair of values apply to the phase diagrams in Figure 2, frames b and c, while the second applies to diagram d.

As shown by these diagrams, at low temperatures $T < T^*$, all monomers are effectively hydrophilic and are found in a homogeneous phase. Even for small values of the association energy g, as in frame c, it is clear that the lower boundary of the coexistence region lies close to the $T = T^*$ line. As shown in frame d, the boundary comes closer to this line for sharper transitions of the local state of the polymer. In all the activated cases the line separating the gel and sol regions can be approximated, as noted in the theoretical section, by two lines: a vertical asymptote of roughly constant concentration and a horizontal low-temperature boundary with an approximately constant temperature near in value to, but lower than, the activation temperature.

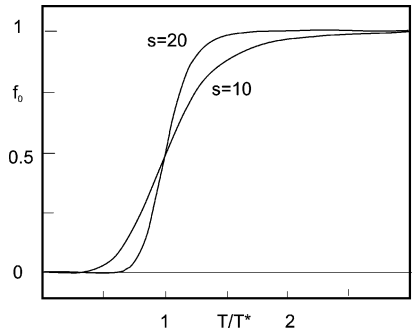

Figure 3. Activated monomer fraction in the low concentration limit f_0 for values of the dissociation entropy and association energy of $s = 10.0$, $E = -10.0T^*$ and $s = 10.0$, $E = -10.0T^*$. These values correspond to the cases in Figure 2, parts b,c and d, respectively. The width of the region where the largest part of the change occurs has size inversely proportional to s and E/T^*.

Measurements of the heat capacity of samples of specified polymer content have been used to detect the gel–sol transition and phase separation.[5,11,43] In Figure 4, we present examples of the heat capacities predicted by the theory for two of the systems of Figure 2. The top panel corresponds to Figure 2b, with $s = 10$, $E = -10T^*$, $g = -1.0T^*$, and concentration $\varphi = 0.13$ (top). For this concentration there is a range of temperatures for which the system is in the coexistence region. Entrance or exit to/from this region leads to singularity in the heat capacity in the form of a discontinuity. We can define an excess heat capacity contribution due to phase separation by subtracting the heat capacity of the meta- or unstable states defined by the same temperature and concentrations from the total heat capacity of the coexisting phases. This excess contribution exhibits the singularities mentioned above. These singu-

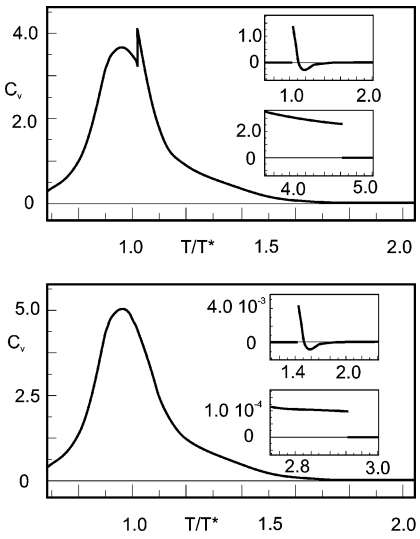

Figure 4. (top) Heat capacity for the system shown in Figure 2b, with parameters $s = 10.0$, $E = -10.0T^*$, and $g = -1.0T^*$, for concentration $\varphi = 0.13$. (bottom) Heat capacity for the system shown in Figure 2c, with parameters $s = 10$, $E = 10T^*$, and $g = -0.2T^*$, for concentration $\varphi = 0.02$ (bottom). In each case the main panel shows the total heat capacity. The insets show the excess heat capacity that arises from crossing the boundary of the coexistence region. The top insets correspond to entrance to the coexistence region and the bottom insets to exit from the region. These excess heat capacities exhibit a singularity in the form of a discontinuity. In the bottom figure these singular contributions are minuscule.

larities are shown in the insets to the main panels of Figure 4. The bottom panel of Figure 4 shows results for the heat capacity of the system in Figure 2c, with $s = 10$, $E = 10T^*$, and $g = -0.2T^*$, for a concentration $\varphi = 0.02$. In this case the excess heat capacity is very small, and its effect is effectively invisible in the main panel. Note the scales in these figures compared to the main signature of the heat capacity.

The examples presented above are typical of the behavior of the system for most values of the parameters of the model. The main features of the heat capacity curves are as follows. It can be shown that there are no special features at the gel transition point in the heat capacity. This is a property of the model, and using a different free energy functional may lead to the appearance of a distinctive feature. It is clear that the main component of the heat capacity corresponds to the internal activation process that transforms the monomers from hydrophilic to hydrophobic. The height of its peak is approximately concentration independent. The position of the peak is thus controlled only by the values of the internal conversion parameters s and E. This shape is relatively broad even for the values used in the examples. For transitions observed in real systems, a narrower shape will indicate large values of the activation energy that can only be realized if the activation is a multimolecule phenomenon, that is, if several water molecules at once change their state of association with the monomer. The phase separation is signaled by a discontinuity in the specific heat, but as in the second example of Figure 4, its effect might be overshadowed by the activation part of the heat capacity. Furthermore, the exothermal behavior after the phase transition produces a second signature of the phase separation. In polydisperse systems, and in situations in which kinetics effects play an important role, the convolution of these signatures by the measuring apparatus might

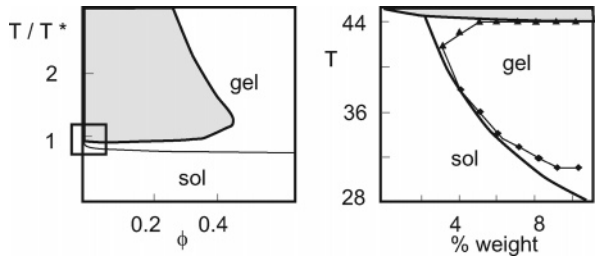

Figure 5. On the left panel, a theoretical phase diagram for parameter values of $N = 3000$, $s = 17$, $E = -17$, and $g = -1.5$. Marked by a rectangle is the region of convergence of gel, sol, and phase separated regions. On the right, a comparison of this region with experimentally determined boundaries for p-(NIPAAm-*co*-acrylic acid) obtained by Han and Bae.[14] The units in the left panel correspond to the dimensionless model variables. Temperatures in °C in the right panel.

lead to the effective detection of only an exothermic or endothermic feature. As we are considering partially water-soluble polymers, the exit temperature from the two-phase region might lie above the water boiling temperature for many concentrations and thus be unobservable.

V. Comparison with Known LCST Gel Systems

The results obtained from analysis and numerical evaluation of the proposed model with different values for the model parameters lead to the identification of features common to the phase structure and calorimetric properties of experimental polymer systems. These features are (i) the presence of a relatively flat, almost concentration independent, monomer activation and transition into a gel state at low temperatures, (ii) the small concentration dependence of the gel transition, such that the transition temperature decreases with concentration, (iii) the presence of a transition into an immiscibility region at temperatures above the gel transition, also with a relatively weak concentration dependence, and (iv) a qualitatively distinct contribution to the heat capacity from internal transformation (monomer activation) that is larger and different in shape than the contributions associated with gel formation and phase separation.

The main examples of systems exhibiting these features are N-substituted acrylamide polymers. A full determination of the phase diagrams of these systems over a large range of temperatures and concentrations is still lacking. Beyond the qualitative agreement of the features mentioned above, direct comparisons of theory and experiment are thus limited to relatively small regions of the phase diagrams. Figure 5 shows, on the left, a theoretical phase diagram for parameter values of $N = 3000$, $s = 17$, $E = -17$, and $g = -1.5$ and, on the right, a superposition of the diagram over experimental data on p-(NIPAAm-*co*-acrylic acid) obtained by Han and Bae.[14] The experimental data range corresponds to the region of convergence of gel formation and phase separation marked by a rectangle in the left panel. The overlap was obtained considering groups of five monomers as the statistical unit and using the molar ratio of these units to water as the volume fraction. The phase properties of the same copolymer, with different composition ratios, have also been indirectly determined though calorimetric experiments,[11] with similar results. For several of these systems, the width of the transition region $\Delta T/T^*$ can be estimated to be of order ~ 0.1. It has been argued[20,26] that, per water molecule, the

destruction of a hydrogen bond produces an entropic change of approximately $\Delta s \approx 3$. The net entropic change s required to obtain widths of order 0.1 is of magnitude ~10−20. The activation of a monomer or statistical unit would then require the freeing of several water molecules, as expected.

In the comparison in Figure 5, both the experimental data and the theory show an almost constant phase separation temperature in a range of concentrations in which the gel transition temperature does change. The theory predicts a smooth boundary for the coexistence region, not affected by the gel transition line. In the experimental data, at the convergence of these boundaries, the gelation does appear to affect the location of the coexistence region. There are many variations in the fit parameters that also produce reasonable agreement with the experimental data. If future experimental data confirm the trend, at larger concentrations, toward an almost constant gel transition temperature, a better fit will be obtained over a larger concentration region by considering a sharper transition process. A sharper process reduces the gap between gelation and phase separation.

Both the triblock copolymer poly(ethylene glycol)−poly(DL-lactic acid-*co*-glycolic acid)−poly(ethylene glycol) (PEG−PLGA−PEG)[5,44] and Poloxamer 407[43] exhibit both gelation and LCST-type phase separation. Their phase diagrams have similar features to those of the theory and the NIPAAm copolymers. However, these polymers also form micelles within the range of temperatures at which gelation occurs. In these cases, the micelles can be though of as the basic units of the system, instead of the individual polymer molecules. The activation process corresponds to structural changes that allow the association of pairs of micelles. With these identifications, the theory presented here should show general agreement with the properties of these systems. The region of activation, gelation, and phase separation for these systems is also relatively narrow, and the width of their transition is also of order $\Delta T/T^* \sim 0.10$.

As with the phase diagrams, reported calorimetric properties of these polymers have not been acquired systematically throughout large ranges of temperature and concentrations, but existing data do qualitatively match the results of the theory. In particular, we point out the observation of endothermic peaks associated with monomer activation and exothermic peaks associated with phase separation in p-(NIPAAm-*co*-Aac).[11]

VI. Discussion

The model considered in this article uses a small number of parameters and well-known theoretical approximations to exhibit a set of particular phenomenological features of gel-forming LCST systems. These features, listed in section V, arise from the main assumption of this article, that with increasing temperature there is a sharp *local* internal conversion of monomers into associative states. We have shown qualitative agreement between the model predictions and features of known experimental systems. The width of the transition in experimentally determined phase diagrams can be used to determine bounds on the values of the parameter of the model. Below, we discuss modifications to theory that might be necessary to obtain more precise agreement between the theory and experimental data.

Considerations of the structure of the polymer chains suggest a few modifications to the free energy functional used. First, it is possible to consider that not every single monomer is capable of association; in this case, the fraction of active monomers should have a ceiling $f_M < 1$, set by the composition of the polymer chains. This change affects both the conditions for gel formation and the maximum values of the association energies in the gel state. Furthermore, if the polymer is composed of two different types of chain segments[1] with different solution properties, the average χ parameter ought to have a distinctive component arising from the nonassociative monomers.

In using the standard free energy form F_{sol} from eq 6 for the solution properties of the polymer plus solvent system, we have implicitly chosen a scale for the values of the third virial coefficient. Again, more detailed considerations of the local gel structures formed might require phenomenological modifications for this term. For example, it is possible to consider cases in which pairs of polymer chains are strongly entwined or might form a large number of self-contacts.[29] In both of these extreme cases, there are strong correlations between the states of associations of monomers in the same chain, and these changes ought to be reflected in the values of the virial coefficients appearing in the free energy and even in the effective number of association contacts that a polymer chain may have.

References and Notes

(1) Chen, G. H.; Hoffman, A. S. *Nature (London)* **1995**, *373*, 49.
(2) Jeong, B.; Kim, S. W.; Bae, Y. H. *Adv. Drug Del. Rev.* **2002**, *54*, 37.
(3) Gutowska, A.; Jeong, B.; Jasionowski, M. *Anat. Rec.* **2001**, *263*, 342.
(4) Kim, S.; Healy, K. E. *Biomacromolecules* **2003**, *4*, 1214.
(5) Jeong, B.; Choi, Y. K.; Bae, Y. H.; Zentner, G.; Kim, S. W. *J. Controlled Release* **1999**, *62*, 109.
(6) Jeong, B.; Kibbey, M. R.; Birnbaum, J. C.; Won, Y. Y.; Gutowska, A. *Macromolecules* **2000**, *33*, 8317.
(7) Serres, A.; Baudys, M.; Kim, S. W. *Pharm. Res.* **1996**, *13*, 196.
(8) Zhang, K.; Wu, X. Y. *Biomaterials* **2004**, *25*, 5281.
(9) Bromberg, L. E.; Ron, E. S. *Adv. Drug Del. Rev.* **1998**, *31*, 197.
(10) Zhang, J. T.; Huang, S. W.; Cheng, S. X.; Zhuo, R. X. *J. Polym. Sci., Part A* **2004**, *42*, 1249.
(11) Vernon, B.; Kim, S. W.; Bae, Y. H. *J. Biomater. Res.* **2000**, *51*, 69.
(12) An, Y. H.; Webb, D.; Gutowska, A.; Mironov, V. A.; Friedman, R. J. *Anat. Rec.* **2001**, *263*, 336.
(13) Cho, J. H.; Kim, S. H.; Park, K. D.; Jung, M. C.; Yang, W. I.; Han, S. W.; Noh, J. Y.; Lee, J. W. *Biomaterials* **2004**, *25*, 5743.
(14) Han, C. K.; Bae, Y. H. *Polymer II* **1998**, *39*, 2809.
(15) Stile, R. A.; Healy, K. E. *Biomacromolecules* **2001**, *2*, 185.
(16) Stile, R. A.; Healy, K. E. *Biomacromolecules* **2002**, *3*, 591.
(17) Lee, K. Y.; Mooney, D. J. *Chem. Rev.* **2001**, *101*, 1869.
(18) Finney, J. L.; Bowron, D. T.; Daniel, R. M.; Timmins, P.; Roberts, M. A. *Biophys. Chem.* **2003**, *105*, 391.
(19) Bae, Y. C.; Lambert, S. M.; Soane, D. S.; Prausnitz, J. M. *Macromolecules* **1991**, *24*, 4403.
(20) Moelbert, S.; De los Rios, P. *Macromolecules* **2003**, *36*, 5845.
(21) Head-Gordon, T. *Proc. Natl. Acad. Sci. U.S.A.* **1995**, *92*, 8308.
(22) Wheeler, J. C. *J. Chem. Phys.* **1975**, *62*, 433.
(23) Walker, J. S.; Vause, C. A. *J. Chem. Phys.* **1983**, *79*, 2660.
(24) Muller, N. *Acc. Chem. Res.* **1990**, *23*, 23.
(25) Lee, B.; Graziano, G. *J. Am. Chem. Soc.* **1996**, *118*, 5163.
(26) Silverstein, K. A. T.; Haymet, A. D. J.; Dill, K. A. *J. Chem. Phys.* **1999**, *111*, 8000.
(27) Schild, H. G.; Tirrell, D. A. *J. Phys. Chem.* **1990**, *94*, 4352.
(28) Flory, P. J. *Principles of Polymer Chemistry*; Cornell University Press: Ithaca, NY, 1953.
(29) Semenov, A. N.; Rubinstein, M. *Macromolecules* **1998**, *31*, 1373.
(30) Erukhimovich, I.; Ermoshkin, A. V. *J. Chem. Phys.* **2002**, *116*, 368.

(31) Erukhimovich, I.; Thamm, M. V.; Ermoshkin, A. V. *Macromolecules* **2001**, *34*, 5653.
(32) Tanaka, F. *Phys. Rev. Lett.* **1992**, *68*, 3188.
(33) Tanaka, F.; Ishida, M. *Macromolecules* **1999**, *32*, 1271.
(34) Kumar, S. K.; Douglas, J. F. *Phys. Rev. Lett.* **2001**, *8718.*
(35) Gujrati, P. D.; Bowman, D. *J. Chem. Phys.* **1999**, *111*, 8151.
(36) Tonsing, T.; Oldiges, C. *Phys. Chem. Chem. Phys.* **2001**, *3*, 5542.
(37) Bershtein, V. A. *Differential Scanning Calorimetry of Polymers: Physics, Chemistry, Analysis, Technology*; Ellis Horwood: New York, 1994.
(38) Arnauts, J.; Decooman, R.; Vandeweerdt, P.; Koningsveld, R.; Berghmans, H. *Thermochim. Acta* **1994**, *238*, 1.
(39) Koningsveld, R.; Stockmayer, W. H.; Nies, E. *Polymer Phase Diagrams: A Textbook*; Oxford University Press: New York, 2001.
(40) Tanaka, F. *Macromolecules* **1989**, *22*, 1988.
(41) Tanaka, F.; Matsuyama, A. *Phys. Rev. Lett.* **1989**, *62*, 2759.
(42) Privalov, P. L.; Gill, S. J. *Adv. Protein Chem.* **1988**, *39*, 191.
(43) Cabana, A.; Ait-Kadi, A.; Juhasz, J. *J. Colloid Interface Sci.* **1997**, *190*, 307.
(44) Lee, D. S.; Shim, M. S.; Kim, S. W.; Lee, H.; Park, I.; Chang, T. Y. *Macromol. Rapid Commun.* **2001**, *22*, 587.

MA047895A